Received: 22 May 2023 | Accepted: 21 December 2023

DOI: 10.1111/1365-2435.14523

Functional Ecology | BRITISH ECOLOGICAL SOCIETY

RESEARCH ARTICLE

The hidden costs of resistance: Contrasting the energetics of successfully and unsuccessfully fighting infection

Matthew D. Hall[1] | Ben L. Phillips[2] | Craig R. White[1] | Dustin J. Marshall[1]

[1]School of Biological Sciences, Monash University, Melbourne, Victoria, Australia

[2]School of Molecular and Life Sciences, Curtin University, Perth, Western Australia, Australia

Correspondence
Matthew D. Hall
Email: matthew.hall@monash.edu

Funding information
Australian Research Council, Grant/Award Number: DP160101730 and FT180100248

Handling Editor: Amy Pedersen

Abstract

1. Exposure to a pathogen is predicted to lead to increased energy use as hosts attempt to activate a costly immune system and repair damaged tissue. To meet this demand, metabolic rates, which capture the rate at which a host can use, transform and expend energy, are expected to increase. Yet for many host–pathogen systems, metabolic rates after encountering a pathogen are just as likely to decrease as increase, suggesting that increased energy expenditure may not always be best for fighting infection.
2. Diverging metabolic trajectories have been previously attributed to the different pathways that specific pathogen classes, such as bacteria or viruses, induce in a host. Here, we test how the magnitude and direction of metabolic change following pathogen exposure might also depend on whether a host has cleared infection or is instead fighting to reduce pathogen burden, as well as interactions between host and pathogen genotypes of a single host–pathogen system.
3. Using a model system, *Daphnia* magna and its bacterial pathogen, we quantified changes in mass-independent metabolic rates over a 30-day period for multiple host and pathogen genotypes. We found that the metabolic trajectory of an exposed host diverged quickly during the infection process. For hosts that were exposed to a pathogen and resisted infection, their mass-independent metabolic rates remained suppressed long after exposure, leading to a sustained reduction in total energy use compared to unexposed animals. The reverse was true for hosts in which the pathogen was able to establish an infection.
4. Underlying these changes were differences in the energetic burden that each pathogen genotype imposed on its host, as well as changes in the way host genotype and the outcome of infection shaped underlying scaling relationships between host body mass and metabolic rates. Our results demonstrate how variation in an organism's metabolic rate and overall energy use can arise from within a single host–pathogen encounter and depend on the likelihood of pathogen clearance, as well as the within-species genetic variability of both hosts and pathogens.

KEYWORDS
costs of resistance, *Daphnia magna*, energy expenditure, host–pathogen interactions, immunity, metabolic rate, metabolic scaling, *Pasteuria ramosa*

1 | INTRODUCTION

Under the threat of infection, a host is required to activate a costly immune system, sequester essential nutrients away from the invading pathogen and potentially repair damaged tissue (Schmid-Hempel, 2011; Siva-Jothy et al., 2005). Exposure to a pathogen is therefore predicted to lead to increased energy use as organisms strive to meet the added energetic demands of fighting infection (Schmid-Hempel, 2003; Sheldon & Verhulst, 1996). Owing to the finite pool of resources that an organism can invest in traits, this allocation of energy towards host resistance is predicted to use resources that might have otherwise been available for other functions, leading to trade-offs between the immune function and other condition-dependent life-history traits (Labbé et al., 2010; Lochmiller & Deerenberg, 2000; Sandland & Minchella, 2003; Zuk & Stoehr, 2002). Yet despite the importance that these presumed costs hold for host–pathogen theory (Antonovics & Thrall, 1994) and the field of ecological immunity in particular (Sheldon & Verhulst, 1996), attempts to quantify the energetic demands of fighting infection have yielded conflicting results (Arnold et al., 2013; Lochmiller & Deerenberg, 2000; Robar et al., 2011), suggesting that increasing energy expenditure may not always be best for fighting infection (Hite et al., 2019; Nørgaard et al., 2021).

In general, the rate at which a host might use, transform and expend energy is described by its metabolic rate (Brown et al., 2004). Under the assumption that pathogens induce defences in a host that are energetically expensive (but see Rigby et al., 2002), a common prediction is that metabolic rates will increase following exposure to a pathogen (akin to the 'increased-intake hypothesis', Bennett & Ruben, 1979; Nilsson, 2002). Across many host–pathogen systems, however, the change in metabolic rates after encountering a pathogen appears just as likely to decrease as increase (reviewed in Robar et al., 2011). It has been suggested that a lower metabolic rate might allow for more energy to be allocated towards other fitness enhancing functions such as immune responses (i.e. the 'compensation hypothesis', Larivée et al., 2010; Steyermark, 2002). Alternate explanations instead centre on how changes in metabolic rates and total energy vary with the class of pathogen that is invading and the physiological response it elicits in the host (Downs et al., 2013; Wang et al., 2016). The metabolic requirements of inflammation, for example, depend on whether the pathogen is a virus or bacteria, leading to the provisioning of food improving a host's resistance against bacterial infection, but at a cost of fighting viral infection (Wang et al., 2016). Ultimately, however, as metabolic rate captures the overall capacity of an organism to do biological work, the energetics of fighting infection will not be the property of either a host or pathogen alone, nor depend solely on the allocation of energy to immune function.

Many aspects of infectious disease, from the probability of infection to aspects of morbidity or mortality, depend on the genotype of the invading pathogen, the genotype of the host and their interaction (Hall et al., 2017; Schmid-Hempel & Ebert, 2003). Fighting infection also depends on multiple defence mechanisms (Hall et al., 2017; Schmid-Hempel & Ebert, 2003). A host, in general, can defend against a pathogen by reducing burden (preventing an infection or limiting pathogen growth) or by improving tolerance (minimising the damage a pathogen causes (Råberg et al., 2009)), but underlying each are a range of behaviours, physical barriers, chemical and cellular processes. Some induced responses likely require an increased supply of energy and elevated metabolic rates as a result, like avoiding pathogens through behavioural modifications (Giorgi et al., 2001; Luong et al., 2017), inducing a fever (Sauer et al., 2019) or activating macrophages (Kolliniati et al., 2021). Infected hosts, however, can also enter energy-saving states that suppress metabolic rates, such as via anorexia or lethargy (Adelman & Martin, 2009; Bashir-Tanoli & Tinsley, 2014; Hart, 1988; Hite et al., 2019), to deprive pathogens of essential nutrients or prioritise maintaining host health over controlling pathogen burden (Ganeshan et al., 2019). As a result, the metabolic costs of fighting infection are unlikely to be shared equally along the entire infection process (akin to Rigby et al., 2002), and will depend on both host and pathogen genotype within a given population, not just between different types of pathogens (see Olive and Sassetti (2016) for a review of metabolic crosstalk between hosts and pathogens).

Using the crustacean *Daphnia magna* and its obligate bacterial pathogen *Pasteuria ramosa*, we estimated metabolic rate, via oxygen consumption rates (Gipson et al., 2022; Nørgaard et al., 2021), for 10 compatible host–pathogen genotypic combinations, plus controls. Disease progresses swiftly in this system, with immune activation expected shortly after exposure (Auld et al., 2010; Labbé & Little, 2009), followed by the rapid loss of fecundity and an increase in mortality (Clerc et al., 2015; Gipson & Hall, 2018; Hall et al., 2019). Notably, these characteristics of disease, particularly those that occur early in the infection process (Hall et al., 2017), are defined by strong interactions between host and pathogen genotypes (Carius et al., 2001; Hall & Ebert, 2012; Luijckx et al., 2010). We measured metabolic rates immediately before exposure to the pathogen (Day 10), and then at two subsequent time points that capture the progression of disease (Days 15 and 30). The success of infection was also tracked for all individuals, allowing differences in metabolic rate to be compared between animals that were exposed to a pathogen and yet remained uninfected, presumably due to their ability to resist and clear the infection, versus those that were exposed and subsequently become sick.

With this design, we were able to contrast the energetics of hosts that successfully (exposed and remain uninfected) and

unsuccessfully (exposed and become infected) resisted infection for different host–pathogen combinations. Our goal was to address three key questions: (i) How do mass-independent metabolic rates respond to pathogen exposure and infection, and do the responses differ between host and pathogen genotypes; (ii) does pathogen exposure and subsequent infection alter metabolic scaling with body size and are patterns consistent between these two outcomes; and, (iii) what are the total energetic costs for a host that either successfully or unsuccessfully resisted infection.

2 | MATERIALS AND METHODS

Daphnia magna Straus is a freshwater crustacean found in ponds and lakes throughout Eurasia and North America and reproduces via cyclical parthenogenesis. *Pasteuria ramosa* Metchnikoff 1888 is an endospore-forming bacteria that is exclusively horizontally transmitted, with spores released from the decaying cadaver of infected animals. Infection by this pathogen results in a severe loss of fecundity, an increase in body size and a reduction in survival (Ebert et al., 2016; Hall et al., 2019). Up to 20 million spores accumulate in the body cavity and are released upon host death (Clerc et al., 2015; Hall & Ebert, 2012). For this study, we used two host (HU-HO-2 and BE-OMZ-M10, herein HO2 and M10) and five pathogen (C1, C19, C20, C14 and C24) genotypes that are completely compatible and differ strongly in characteristics of the onset and severity of infectious disease (Clerc et al., 2015; Hall & Ebert, 2012; Luijckx et al., 2010). This study did not require animal ethics approval.

Before the experiment, all *Daphnia* clones were maintained under standardised conditions for at least three generations. Animals were raised individually in 100-mL jars filled with 80 mL of artificial media (AdaM; Klüttgen et al., 1994, modified as per Ebert et al., 1998) and kept in a single controlled climate chamber (16:8 light–dark cycle and 20°C, locations rotated daily to minimise positional effects). Animals were fed daily with green algae (*Scenedesmus* sp.), and food levels were increased to meet the growing needs of the animals, from 0.5 million cells per animal per day at birth to 5 million cells per animal per day from age 13 days onwards. Subsequent experiential animals were maintained under identical conditions.

2.1 | Experimental infection trials

A cross-infection experiment was conducted using the two *Daphnia* genotypes and five different *P. ramosa* genotypes as part of a factorial design. Animals were collected from standardised cultures at birth and placed individually in 60-mL jars filled with 50 mL of *Daphnia* medium. Approximately every 3 days thereafter, the animals were transferred to fresh jars containing 50 mL of artificial media, again maintaining one animal per jar. On Days 11 and 12, for each host genotype, 80 animals received 30,000 spores of a randomly allocated pathogen genotype (i.e. 60,000 spores in total) and 50 animals received the equivalent volume of a control (placebo suspension produced from uninfected *Daphnia*). Survival was monitored daily, and the infection status of each individual was recorded based on the reddish coloration of an otherwise transparent organism, which is characteristic of infection by *P. ramosa* (Ebert et al., 2016).

2.2 | Metabolic rate measurements

Oxygen consumption rates (VO_2) were used as a proxy for metabolic rate. Measurements were conducted at three ages: Day 10 (pre-exposure to the pathogen), Day 15 (3–4 days post-exposure) and Day 30 (18–19 days post-exposure). Animals were placed individually into 5-mL glass vials full of autoclaved artificial media and containing a non-consumptive oxygen sensor spot. For each airtight vial, VO_2 was measured via a 24-channel reader (SDR SensorDish Reader, PreSens Precision Sensing GmbH, Germany) with multiple readers run in parallel (up to 6 × 24-channel readers at a time). The sensor spots were first calibrated with air-saturated artificial media and water containing 2% sodium sulphite. All assays of oxygen consumption were performed over 90 min in complete darkness and in a temperature-controlled room (21°C). Immediately following the assays, the body size of each animal was measured and converted to dry weight (herein µg, following Yashchenko et al., 2016).

Each set of 24 vials contained 20 animals, along with four blank controls containing only sterile artificial media. For each animal, VO_2 was calculated from the change in oxygen saturation over time (% h^{-1}) as per White et al. (2011): $VO_2 = -[(m_a - m_c)/100] \times V \times \beta O_2$, where m_a is the rate of change of oxygen saturation for an experimental animal, m_c is the per-run average rate of change for the blank controls, βO_2 is the oxygen capacitance of air-saturated water at 21°C (6.40, Cameron, 1986) and V is the water volume of the vials (0.005 L). The parameters m_a and m_c were estimated using the *LoLinR* package in R (Olito et al., 2017), which uses local linear regressions to objectively estimate the monotonic rates from oxygen consumption data. VO_2 estimates (in mL O_2 h^{-1}) were then converted to metabolic rate (microjoules h^{-1}) using the calorific conversion factor of 20.08 J mL^{-1} O_2 (Schmidt-Nielsen, 1990).

2.3 | Replication statement

In total, there were 10 treatment groups (two host genotypes × 5 pathogen genotypes), with 80 animals initially assigned to each, plus 48 unexposed controls per host genotype (896 animals). See Table 1 for a summary of the scale of replication in this study. Of the 896 animals initiated in the study, not all were available for the three metabolic assays (Days 10, 15 and 30), as they either died before the end of the study or were excluded from an assay due to sampling errors. We could estimate the metabolic rate of 822 animals at

TABLE 1 Replication statement.

Scale of inference	Scale at which the factor of interest is applied	Number of replicates at the appropriate scale
Age-specific metabolic rate estimates	Individual	Per host genotype: initially 80 animals assigned to each pathogen genotype, plus 48 unexposed controls

Note: The level of interference is the age-specific metabolic rate estimates (and their derivatives). The factors of interest are host genotype (2 levels: M10 or HO2), pathogen genotype (5 levels: C1 etc.) or control animals, and when exposed to pathogen, exposure outcome (2 levels: exposed and infected, exposed and uninfected). The factors of interest were applied to individual *Daphnia*, raised individually from birth in small jars.

Day 10 (90 controls, 208 exposed and uninfected, 524 exposed and infected), 837 animals at Day 15 (90 controls, 204 uninfected, 543 infected) and 646 animals at Day 30 (85 controls, 128 uninfected, 433 infected). Total assays were evenly split between the two host genotypes (1148 M10 and 1157 HO2) and five pathogen genotypes (345–437).

2.4 | Statistical analyses

All statistical analyses were performed in R (ver. 4.2.3; R Development Core Team). To understand how metabolic rate relates to the progression of disease, we explored the scaling relationship between metabolic rate (Y, with units of μJ/h) and body mass (M, with units of μg) of the experimental animals as described by the power function $Y = aM^b$, where b is the scaling exponent and a is the normalisation constant (or proportionality constant) that accounts for differences in absolute metabolic rates with respect to mass for a given a value (Niklas & Hammond, 2019; White & Kearney, 2014). We first used this power function to derive mass-independent estimates of metabolic rate from the residuals of a non-linear regression of raw metabolic rates on mass, as modelled using the *drc* package (Ritz et al., 2015) and the self-starting power curve function of the *aomisc* package (see github.com/OnofriAndreaPG/aomisc/). Linear mixed-effects models were used to assess if the change in mass-independent metabolic rate depended on the following fixed effects: host genotype (M10 or HO2), pathogen genotype (C1 etc.), the age at which a metabolic measure was taken (age of measure: 10, 20 and 30 days), exposure outcome (whether an exposed individual become infected or not) and their interactions. Animal identity was included as a random effect to account for the multiple estimates available for each individual.

We next assessed the sensitivity of the scaling exponent (b) and the normalisation constant (a) to interactions between host genotypes and exposure outcomes. When both metabolic rate and body mass are log transformed, b and a can be readily estimated as the slope and intercept, respectably, of a linear regression where $\log_{10}Y = \log_{10}a + b\log_{10}M$ (White & Kearney, 2014). Metabolic rates were analysed using this log–log framework via a linear mixed-effect analysis of covariance via the *lmer* package (Bates et al., 2015), with host genotype (M10 or HO2), exposure treatments (controls, exposed and uninfected, exposed and infected), $\log_{10}$ mass and their interactions as fixed effects and animal identity as a random effect (to account for the multiple age-specific estimates of each individual). As per an analysis of covariance, significant interactions between a factor (host genotype or exposure outcome) and the $\log_{10}$ mass covariate indicated a change in slope between the treatment levels and thus scaling exponents. We compared any change in slope between each level of a treatment using the package *emmeans* (see github.com/rvlenth/emmeans).

Finally, we estimated the overall change in energy use before and after exposure to a pathogen for each treatment combination. Initial energy use was estimated simply as the VO_2 estimates (in $mL\,O_2\,h^{-1}$) taken for each individual immediately before they were exposed to a pathogen or placebo suspension (10 days old, see above). Total energy use after pathogen exposure was subsequently estimated by calculating the difference in VO_2 measures throughout the experimental period. We then used the trapezoid method to calculate the total area under the curve for the 20 days following exposure. We analysed both traits (square root transformed) with host genotype (M10 or HO2), exposure treatments (controls, exposed and uninfected, exposed and infected) and their interaction as fixed effects, ignoring for now the effects of individual pathogen genotypes (which prohibited including controls as a level of the exposure factor). In a separate analysis, we explored how pathogen genotype (C1 etc.), interacting with both host genotype and exposure outcome (exposed and uninfected, exposed and infected), shaped energy use after exposure. In both cases, where a global test was significant, such as a main effect, post hoc comparisons between treatment means were then conducted via uncorrected pairwise t-tests as implemented via the package *emmeans*.

3 | RESULTS

3.1 | The metabolic costs of defending against infection extend long after exposure

Mass-independent metabolic rates were typically highest in infected animals by Day 30 (Figure 1, exposed and infected). In contrast, most animals that were exposed to a pathogen and were able to successfully clear the infection showed a decline in mass-independent

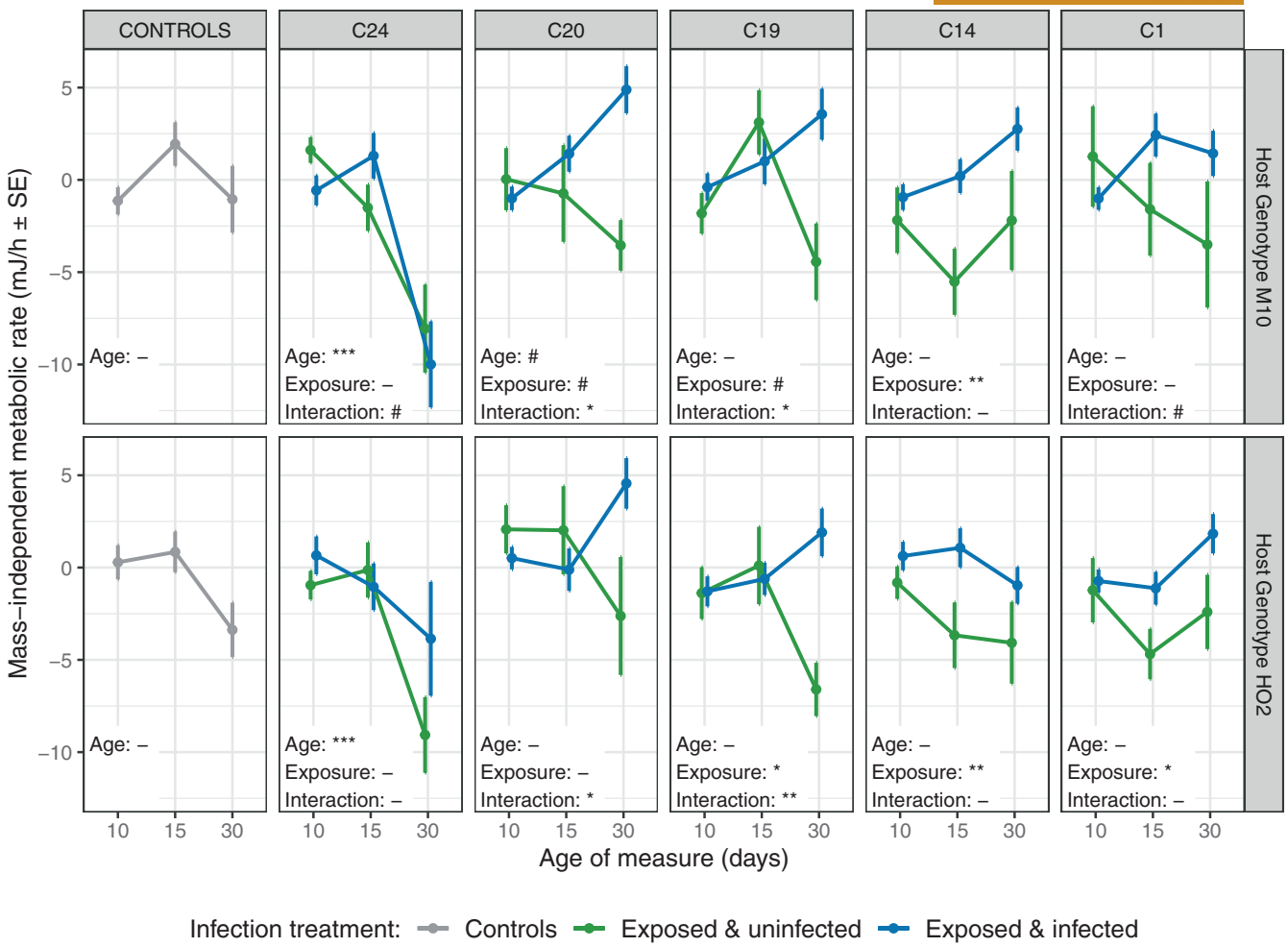

FIGURE 1 The change in mass-independent metabolic rates before (Day 10) and after (Days 15 and 30) pathogen exposure for (i) animals that were exposed to a pathogen and remained uninfected; (ii) animals that were exposed to a pathogen and became infected; and for reference, (iii) control animals that were never exposed to the pathogen. Results are partitioned by host (M10 and HO2) and pathogen (C24 etc.) genotypes. Within each panel are the results of the corresponding linear mixed-effect model (*$p<0.05$, **$p<0.01$, ***$p<0.001$). Mass-independent estimates of metabolic rate were extracted from the residuals of a model of metabolic rate (μJ/h) and body mass (μg) as estimated via a non-linear power curve model.

metabolic rates over the same period (Figure 1, exposed and uninfected). By Day 30, on average, the metabolic response of exposed and infected animals was 4.40 mJ/h higher (±1.21 SE, $p<0.001$) than the matched control animals, compared to that of the exposed and uninfected animals, which was 3.01 mJ/h lower (±1.32 SE, $p=0.024$) than controls. Although an increase in body size is often associated with infection in this system (e.g. Hall et al., 2019; but see Supporting Information), body mass was not systematically different between the exposure treatments (control, exposed and uninfected, exposed and infected) over the experimental period for both the M10 ($F_{2,1145}=2.73$, $p=0.066$) and HO2 genotypes ($F_{2,1154}=0.13$, $p=0.878$). Correlated changes in body mass were thus not solely driving the variation in mass-independent metabolic rates that occurred soon after pathogen exposure (see Figures S1 and S2 which show the overlap in overall and age-specific body mass between the treatment groups).

Overall, any change in mass-independent metabolic rates over time was found to depend on an interaction between exposure outcome and the underlying pathogen genotype (a three-way interaction with age, Table 2). Host genotype contributed little to these changes (all terms $p>0.05$). In most cases, mass-independent metabolic rates increasingly diverged between the exposure treatments as infection progressed, but each pathogen genotype varied in the rate at which these changes occur. Only for pathogen C24 did the mass-independent metabolic rates universally decline after pathogen exposure, irrespective of whether an animal was infected or not. However, the three-way interaction term remained ($\chi^2_6 = 18.25$, $p=0.006$) after excluding this pathogen, indicating that the metabolic trajectories of a host after exposure are likely to be shaped by the genotype of the pathogen, and not biased by this one treatment.

3.2 | Pathogen exposure changes metabolic scaling exponents

Underlying the distinct metabolic trajectories of successfully and unsuccessfully resisting infection appear to be differences in the

allometric scaling relationship between metabolic rate and body mass. Using a log–log regression framework, we found both the normalisation constants (log–log intercept) and scaling exponents (log–log slope) to vary with the outcome of pathogen exposure (exposure main effect: $\chi^2_2 = 45.09$, $p < 0.001$; Log_{10} mass × exposure: $\chi^2_2 = 53.33$, $p < 0.001$) and, to a lesser extent, the host genotype (host main effect: $\chi^2_2 = 4.99$, $p = 0.026$; Log10 mass × host: $\chi^2_1 = 5.15$, $p = 0.023$). There was no evidence for either parameter to depend on interactions between host genotypes and infection treatments (host × exposure term: $\chi^2_2 = 0.08$, $p > 0.05$; Log_{10} mass × host × exposure: $\chi^2_2 = 0.05$, $p > 0.05$).

Examination of the separate regression coefficients (Table 3) shows that animals that were exposed and remained resistant to infection had a lower scaling exponent than the control animals (0.48 vs. 0.62), whereas the reverse was true for animals that become infected by the pathogen (0.72 vs. 0.62). No further differences in scaling exponents were found between the five pathogen genotypes in either the animals that were exposed and remained uninfected (M10: $\chi^2_4 = 4.98$, $p > 0.05$; HO2: $\chi^2_4 = 1.59$, $p > 0.05$) or the animals that were exposed and became infected (M10: $\chi^2_4 = 7.95$, $p > 0.05$; HO2: $\chi^2_4 = 8.42$, $p > 0.05$). The full results of the original two-factor analysis of covariance are shown in Table S1 and Figure S2.

TABLE 2 Linear mixed-effects analysis for the change in mass-independent metabolic rate with increasing age, as partitioned by host, pathogen and infection outcome.

Effect	χ^2	df	*p*-value
Host genotype	0.384	1	0.535
Pathogen genotype	21.908	4	<0.001***
Age of measure	11.241	2	0.004**
Exposure outcome	26.412	1	<0.001***
Host × Pathogen	4.568	4	0.335
Host × Age	1.418	2	0.720
Host × Exposure	0.004	1	0.492
Pathogen × Age	39.206	8	<0.001***
Pathogen × Exposure	4.225	4	0.376
Age × Exposure	24.102	2	<0.001***
Host × Pathogen × Age	8.955	8	0.346
Host × Pathogen × Exposure	2.562	4	0.634
Host × Age × Exposure	2.310	2	0.315
Pathogen × Age × Exposure	21.114	8	0.007**
Host × Pathogen × Age × Exposure	6.229	8	0.622

Note: Fixed effects include host genotype (M10 or HO2), pathogen genotype (C1 etc.), the age at which a metabolic measure was taken (age of measure: 10, 20 and 30 days), exposure outcome (whether an exposed individual become infected or not) and their interactions (Type III, *$p < 0.05$, **$p < 0.01$, ***$p < 0.001$). Animal identity was included as a random effect ($\sigma = 1610$).

3.3 | Total energy use varies with infection success and pathogen genotype

Overall energy use by a host depended on the outcome of pathogen exposure as well as the genotype of the infecting pathogen (Figure 2). To estimate the total energy use of a host, we calculated the difference in VO_2 estimates of individuals from Day 10 (before exposure occurred) and beyond. Exposure and subsequent infection by a pathogen (pooling across pathogen genotypes) led to an increase in total energy use relative to control animals, whereas hosts that were exposed but cleared the pathogen had much lower levels of energy use overall (Figure 2b, Exposure effect: $F_{2,613} = 24.777$, $p < 0.001$; see Table S2). The observed changes in energy use were not driven by systematic differences among the individuals allocated to each exposure treatment, as we observed no significant differences in oxygen consumption rates (initial VO_2, Figure 2a) among these treatment groups before exposure to a pathogen (Exposure effect: $F_{2,816} = 1.503$, $p = 0.222$), other than slightly higher estimates for host genotype HO2 (Host effect: $F_{2,816} = 50.857$, $p < 0.001$; initial VO_2: M10 = 0.080 ± 0.002; HO2 = 0.094 ± 0.002, see also Table S2).

TABLE 3 Summary of scaling coefficients ($a \pm SE$) and exponents ($b \pm SE$) for metabolic rate and mass of different host genotypes and exposure outcomes across ontogeny (ages 10–30 days).

Context	*n*	Coefficient (*a*)	Scaling exponent (*b*)	*p*-value, $b \neq 0$	*p*-value, $b \neq 1$	*p*-value, $b \neq 0.75$
Average differences among host genotypes (pooling exposure outcomes)						
Genotype M10	1148	1780 (±178)	0.569 (±0.022)	<0.001***	<0.001***	<0.001***
Genotype HO2	1157	2529 (±307)	0.489 (±0.027)	<0.001***	<0.001***	<0.001***
Average differences among exposure outcomes (pooling host genotypes)						
Control	265	2762 (±514)	0.474 (±0.041)	<0.001***	<0.001***	<0.001***
Uninfected	540	2865 (±357)	0.450 (±0.028)	<0.001***	<0.001***	<0.001***
Infected	1500	1207 (±89)	0.664 (±0.017)	<0.001***	<0.001***	<0.001***

Note: Estimates were obtained using the log–log linear transformed relationship as implemented in a linear mixed-effect model, where $\log_{10}$ metabolic rate = $\log_{10} a + b \times \log_{10}$ mass, with host genotype and exposure outcomes as interacting fixed effects and animal identity as the random effect. Wald tests were used to assess whether the scaling exponent was statistically different to 0, 0.75 or 1, and *n* refers to the number of mass and metabolic rate observation pairs for each context (*$p < 0.05$, **$p < 0.01$, ***$p < 0.001$).

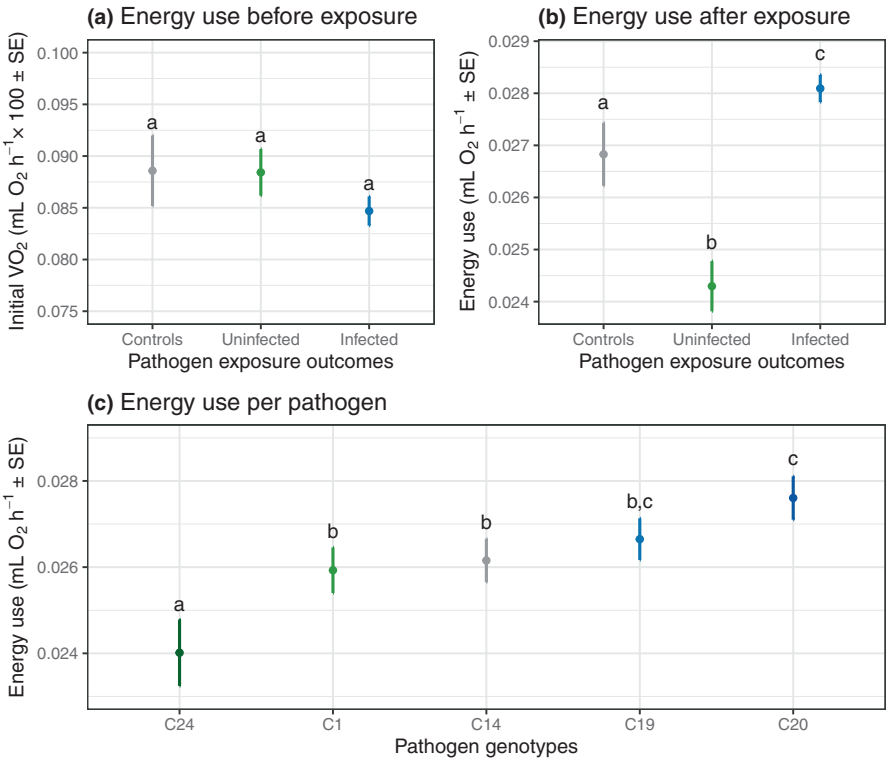

FIGURE 2 Total energy use of a host before and after pathogen exposure. Initial energy use shows the maximal oxygen consumption (VO_2) for hosts before exposure to a pathogen. Energy use after exposure was estimated using the difference between oxygen consumption rates at Day 10 (before pathogen exposure) and beyond. Panels (a) and (b) show the predicted means (± SE) for pathogen exposure outcomes after controlling for host genotype, while panel (c) shows the predicted means for the effect of pathogen genotype, on average, after controlling for the additive effects of exposure outcomes. Treatment levels that share a letter were not significantly different from one another using post hoc comparisons via pairwise *t*-tests.

Partitioning the energy use of exposed hosts by pathogen genotype revealed a significant effect of pathogen genotype ($F_{4,520}=4.118$, $p=0.003$) and infection outcome ($F_{1,520}=30.976$, $p<0.001$). Total energy use was highest in hosts that were successfully infected by a pathogen, and this difference was not dependent on the genotype of the infecting pathogen (pathogen genotype by exposure outcome: $F_{4,520}=1.031$, $p=0.390$). There was no statistically clear effect of host genotype ($F_{1,520}=0.493$, $p=0.482$) nor more complex interactions (see Table S2), such as a host genotype by pathogen genotype interactions ($F_{4,520}=0.327$, $p=0.327$). Instead, across any outcome of pathogen exposure (successful or unsuccessful infections), the energy use of a host was highest when encountering pathogen C20 and lowest when encountering pathogen C24 (Figure 2c).

4 | DISCUSSION

When encountering a pathogen, a host is expected to first focus on killing a pathogen early during infection before turning to controlling the growth of the newly established pathogen or repairing any subsequent damage (Hall et al., 2017; Schmid-Hempel, 2011; Siva-Jothy et al., 2005). Our findings show that the metabolic trajectory of an exposed host diverges quickly during the infection process as a result and is maintained long after the initial encounter (Figure 1). The prolonged increase in mass-independent metabolic rates observed once the pathogen was established is not surprising, given infection is chronic in this system and the pathogen continues to proliferate until causing host death (Clerc et al., 2015; Hall & Mideo, 2018). Mass-independent metabolic rates have also been shown to correlate positively with pathogen load in this study system (Gipson et al., 2022; Nørgaard et al., 2021). Clearing infection, however, is instead expected to occur more rapidly. Relative to the entire process of infection in this system, from a pathogen's initial entry into the host to the termination of infection at host death up to 70 days later (Ebert et al., 2016; Hall et al., 2019), the window for clearance to occur is between a few hours (as inferred by immune assays in *Daphnia*: Auld et al., 2010; Labbé & Little, 2009; supported by changes in colony-forming units for other invertebrate species: Haine et al., 2008) to several days (i.e. until spores begin to appear in the haemolymph from 5 days on, Ebert et al., 2016). Yet here, the mass-independent metabolic rates of hosts that repelled the pathogen remained suppressed long after exposure (Figure 1), leading to a significant and sustained reduction in overall energy use compared to unexposed control animals (Figure 2).

Clearing infection thus appears to induce a long-lasting and, until now, hidden energetic cost. Previous attempts to quantify the potential costs of successfully resisting a pathogen, in this species and others, have centred on documenting induced costs in terms of reduction in fitness components such as fecundity, growth, survival or other factors such as predator avoidance or resistance against different pathogens (Labbé et al., 2010; Lochmiller & Deerenberg, 2000; Sandland & Minchella, 2003; Zuk & Stoehr, 2002). Our results suggest that underlying these fitness costs may be an initial change in the total energy that a host has available to invest in other traits or complete any biological work. This reduction in energetic capacity might arise if a host suppressed their feeding rates in order to deprive a pathogen of the energy needed to successfully establish (Hite et al., 2019) or if they substantially reduced other energetically costly traits, such as activity or growth (sensu White et al., 2022), so

as to better fuel an effective immune response. Measures of host activity and feeding rates are currently not available for hosts that were exposed to a pathogen and successfully resisted infection in this system. However, infection has been shown to reduce activity (Nørgaard et al., 2019a, 2019b) and slightly reduce feeding rates (albeit in a genotype-specific manner, Gipson et al., 2022; Nørgaard et al., 2021), hinting that resistant hosts are most likely behaving differently. However, regardless of the mechanism, our results suggest that the physiological (i.e. inducible) costs incurred by a host, and the potential trade-offs that arise with other fitness components, begin with a reduction in the rate at which hosts can use, transform and expend energy.

Underlying the observed energetics of fighting infection appeared to be changes in the way the metabolic rate of infected and uninfected animals' scales with their mass (Table 1). Although multiple theories exist to explain how variation in metabolic rate should scale allometrically with body mass according to a precise power function (aM^b, where b typically varies between 2/3 and 1 (Glazier, 2005)), many ecological and environmental factors will also cause this relationship to naturally vary (Burton et al., 2011; Glazier, 2010; Pettersen et al., 2018; White et al., 2022; White & Kearney, 2014). Within a single species, for example, simple changes in diet quality have been shown to cause substantial variation in scaling exponents, ranging from 0.45 to 1 (Ruiz et al., 2021). Our results indicate that host–pathogen interactions can also induce variation in metabolic scaling exponents of a similar magnitude (Table 2). Infected hosts experienced an increase in their metabolic scaling exponents from 0.47 to 0.66, with an associated decrease in metabolic level (a, the coefficient or normalisation constant). The reverse pattern was true for hosts that cleared the infection (Table 2). A similar negative covariance between scaling exponents and coefficients is observed in studies that manipulate temperature, with higher temperatures yielding higher coefficients with lower exponents (see Glazier, 2005, 2010 for a mechanistic explanation). In the future, extending these results to also consider the scaling relationship between body mass and immune function (e.g. Downs et al., 2020; Ruhs et al., 2020) will provide a natural complement to understanding how pathogen exposure, immunity and metabolism interact (see Downs et al., 2019).

While previous studies have shown that diverging metabolic trajectories might be expected when a host is infected by different pathogen classes or species (Downs et al., 2013; Wang et al., 2016), we extend these findings to include changes arising as a result of exposure to different pathogen genotypes from within a single species. Pathogen genotype, for example, shaped the relative rates at which mass-independent metabolic rates increased or decreased following exposure to a pathogen (i.e. a pathogen × age × infection interaction), as well as when the metabolic trajectory of uninfected and infected animals diverged (see Figure 1). For some pathogens, such as C14 and C1, the mass-independent metabolic rates of hosts diverged early in the infection process (<5 days post-infection), while others diverged much later (5–20 days post-infection, e.g. C19 and C20). The net result of these changes is that each pathogen genotype imposes a different energetic cost on their host, with hosts infected by the genotypes varying significantly in the total energy that is used across the 20 days that followed pathogen exposure (Figure 2).

Our results demonstrate that variation in the magnitude and direction of change in mass-independent metabolic rates appears to be a natural part of defending against pathogens. Most notably, we found that hosts that successfully resisted infection experienced a sustained reduction in their energetic capacity, and therefore their potential to invest in other components of fitness or do biological work of any kind. The reverse was true for hosts that could not successfully fight off infection. Predictions that metabolic rates should either increase or decrease following pathogen exposure (see Robar et al., 2011), or depend solely on the class of pathogen that is invading, such as bacterial versus viral infection (Downs et al., 2013; Wang et al., 2016), thus oversimplify the energetics associated with the defence against infection. Instead, variation in a host's metabolic rate and energy use will naturally arise from within a single host–pathogen encounter and depend on the likelihood of clearing an infection, as well as the within-species genetic variability of hosts and pathogens. With strong interactions between host and pathogen genotypes a common feature of many disease systems (Hall et al., 2017; Schmid-Hempel & Ebert, 2003), there is ample scope for conflict to arise over how energy is used, transformed and expended. Such conflict may prove integral to the ecology and evolution of host–pathogen interactions and the broader maintenance of variation in energy use and metabolism.

AUTHOR CONTRIBUTIONS

M.D.H., B.L.P., C.R.W. and D.J.M. designed the study. M.D.H. oversaw the laboratory work. M.D.H. analysed the data with input from D.J.M. M.D.H. led the writing of the manuscript. All authors contributed to drafting the manuscript and gave final approval for publication.

ACKNOWLEDGEMENTS

We thank Katharine Prata, Jared Lush and Lindsey Heffernan for assistance in collecting the data and members of the Hall laboratory group for valuable discussion. We also thank Meghan Duffy and one anonymous reviewer for helpful comments on an earlier version of the manuscript. This study was supported by the Centre for Geometric Biology at Monash University and the Australian Research Council (grants FT180100248 to M.D.H. and DP160101730 to M.D.H. and B.L.P.). Open access publishing facilitated by Monash University, as part of the Wiley - Monash University agreement via the Council of Australian University Librarians.

CONFLICT OF INTEREST STATEMENT

D.J.M is a Senior Editor of Functional Ecology but took no part in the peer review and decision-making processes for this paper. None of the authors have any other conflict of interest.

DATA AVAILABILITY STATEMENT

Data are available from the Monash Bridges Digital Repository: https://doi.org/10.26180/24784245 (Hall et al., 2023).

ORCID

Matthew D. Hall https://orcid.org/0000-0002-4738-203X
Ben L. Phillips https://orcid.org/0000-0003-2580-2336
Craig R. White https://orcid.org/0000-0002-0200-2187
Dustin J. Marshall https://orcid.org/0000-0001-6651-6219

REFERENCES

Adelman, J. S., & Martin, L. B. (2009). Vertebrate sickness behaviors: Adaptive and integrated neuroendocrine immune responses. *Integrative and Comparative Biology*, *49*(3), 202–214.

Antonovics, J., & Thrall, P. H. (1994). The cost of resistance and the maintenance of genetic polymorphism in host-pathogen systems. *Proceedings of the Royal Society B: Biological Sciences*, *257*(1349), 105–110.

Arnold, P. A., Johnson, K. N., & White, C. R. (2013). Physiological and metabolic consequences of viral infection in *Drosophila melanogaster*. *Journal of Experimental Biology*, *216*(Pt 17), 3350–3357.

Auld, S. K. J. R., Scholefield, J. A., & Little, T. J. (2010). Genetic variation in the cellular response of *Daphnia magna* (Crustacea: Cladocera) to its bacterial parasite. *Proceedings of the Royal Society B: Biological Sciences*, *277*(1698), 3291–3297.

Bashir-Tanoli, S., & Tinsley, M. C. (2014). Immune response costs are associated with changes in resource acquisition and not resource reallocation. *Functional Ecology*, *28*(4), 1011–1019.

Bates, D., Mächler, M., Bolker, B., & Walker, S. (2015). Fitting linear mixed-effects models using lme4. *Journal of Statistical Software*, *67*(1). https://doi.org/10.18637/jss.v067.i01

Bennett, A. F., & Ruben, J. A. (1979). Endothermy and activity in vertebrates. *Science*, *206*(4419), 649–654.

Brown, J. H., Gillooly, J. F., Allen, A. P., Savage, V. M., & West, G. B. (2004). Toward a metabolic theory of ecology. *Ecology*, *85*(7), 1771–1789.

Burton, T., Killen, S. S., Armstrong, J. D., & Metcalfe, N. B. (2011). What causes intraspecific variation in resting metabolic rate and what are its ecological consequences? *Proceedings of the Royal Society B: Biological Sciences*, *278*(1724), 3465–3473.

Cameron, J. N. (1986). *Principles of physiological measurement*. Academic Press.

Carius, H. J., Little, T. J., & Ebert, D. (2001). Genetic variation in a host-parasite association: Potential for coevolution and frequency-dependent selection. *Evolution*, *55*(6), 1136–1145.

Clerc, M., Ebert, D., & Hall, M. D. (2015). Expression of parasite genetic variation changes over the course of infection: Implications of within-host dynamics for the evolution of virulence. *Proceedings of the Royal Society B: Biological Sciences*, *282*(1804), 20142820.

Downs, C. J., Brown, J. L., Wone, B., Donovan, E. R., Hunter, K., & Hayes, J. P. (2013). Selection for increased mass-independent maximal metabolic rate suppresses innate but not adaptive immune function. *Proceedings of the Royal Society of London B: Biological Sciences*, *280*(1754), 20122636.

Downs, C. J., Dochtermann, N. A., Ball, R., Klasing, K. C., & Martin, L. B. (2020). The effects of body mass on immune cell concentrations of mammals. *The American Naturalist*, *195*(1), 107–114.

Downs, C. J., Schoenle, L. A., Han, B. A., Harrison, J. F., & Martin, L. B. (2019). Scaling of host competence. *Trends in Parasitology*, *35*(3), 182–192.

Ebert, D., Duneau, D., Hall, M. D., Luijckx, P., Andras, J. P., Pasquier, L. D., & Ben-Ami, F. (2016). A population biology perspective on the stepwise infection process of the bacterial pathogen *Pasteuria ramosa* in *Daphnia*. *Advances in Parasitology*, *91*, 265–310.

Ebert, D., Zschokke-Rohringer, C. D., & Carius, H. J. (1998). Within–and between–population variation for resistance of *Daphnia magna* to the bacterial endoparasite *Pasteuria ramosa*. *Proceedings of the Royal Society B: Biological Sciences*, *265*(1410), 2127–2134.

Ganeshan, K., Nikkanen, J., Man, K., Leong, Y. A., Sogawa, Y., Maschek, J. A., Ry, T. V., Chagwedera, D. N., Cox, J. E., & Chawla, A. (2019). Energetic trade-offs and hypometabolic states promote disease tolerance. *Cell*, *177*(2), 399–413.e12.

Giorgi, M. S., Arlettaz, R., Christe, P., & Vogel, P. (2001). The energetic grooming costs imposed by a parasitic mite (*Spinturnix myoti*) upon its bat host (*Myotis myotis*). *Proceedings of the Royal Society of London. Series B: Biological Sciences*, *268*(1480), 2071–2075.

Gipson, S. A. Y., & Hall, M. D. (2018). Interactions between host sex and age of exposure modify the virulence-transmission trade-off. *Journal of Evolutionary Biology*, *31*(3), 428–437.

Gipson, S. A. Y., Pettersen, A. K., Heffernan, L., & Hall, M. D. (2022). Host sex modulates the energetics of pathogen proliferation and its dependence on environmental resources. *The American Naturalist*, *199*(5), E186–E196.

Glazier, D. S. (2005). Beyond the "3/4-power law": Variation in the intra- and interspecific scaling of metabolic rate in animals. *Biological Reviews*, *80*(4), 611–662.

Glazier, D. S. (2010). A unifying explanation for diverse metabolic scaling in animals and plants. *Biological Reviews*, *85*(1), 111–138.

Haine, E. R., Moret, Y., Siva-Jothy, M. T., & Rolff, J. (2008). Antimicrobial defense and persistent infection in insects. *Science*, *322*(5905), 1257–1259.

Hall, M. D., Bento, G., & Ebert, D. (2017). The evolutionary consequences of stepwise infection processes. *Trends in Ecology & Evolution*, *32*(8), 612–623.

Hall, M. D., & Ebert, D. (2012). Disentangling the influence of parasite genotype, host genotype and maternal environment on different stages of bacterial infection in *Daphnia magna*. *Proceedings of the Royal Society B: Biological Sciences*, *279*(1741), 3176–3183.

Hall, M. D., & Mideo, N. (2018). Linking sex differences to the evolution of infectious disease life-histories. *Philosophical Transactions of the Royal Society, B: Biological Sciences*, *373*(1757), 20170431.

Hall, M. D., Phillips, B. L., White, C. R., & Marshall, D. J. (2023). Data from: The hidden costs of resistance: Contrasting the energetics of successfully and unsuccessfully fighting infection. *Monash Bridges Digital Repository*, https://doi.org/10.26180/24784245

Hall, M. D., Routtu, J., & Ebert, D. (2019). Dissecting the genetic architecture of a stepwise infection process. *Molecular Ecology*, *28*(17), 3942–3957.

Hart, B. L. (1988). Biological basis of the behavior of sick animals. *Neuroscience & Biobehavioral Reviews*, *12*(2), 123–137.

Hite, J. L., Pfenning, A. C., & Cressler, C. E. (2019). Starving the enemy? Feeding behavior shapes host-parasite interactions. *Trends in Ecology & Evolution*, *35*(1), 68–80.

Klüttgen, B., Dülmer, U., Engels, M., & Ratte, H. T. (1994). ADaM, an artificial freshwater for the culture of zooplankton. *Water Research*, *28*(3), 743–746.

Kolliniati, O., Ieronymaki, E., Vergadi, E., & Tsatsanis, C. (2021). Metabolic regulation of macrophage activation. *Journal of Innate Immunity*, *14*(1), 51–68.

Labbé, P., & Little, T. J. (2009). ProPhenolOxidase in *Daphnia magna*: cDNA sequencing and expression in relation to resistance to pathogens. *Developmental & Comparative Immunology*, *33*(5), 674–680.

Labbé, P., Vale, P. F., & Little, T. J. (2010). Successfully resisting a pathogen is rarely costly in Daphnia magna. *BMC Evolutionary Biology*, *10*(1), 355.

Larivée, M. L., Boutin, S., Speakman, J. R., McAdam, A. G., & Humphries, M. M. (2010). Associations between over-winter survival and resting metabolic rate in juvenile North American red squirrels. *Functional Ecology*, *24*(3), 597–607.

Lochmiller, R. L., & Deerenberg, C. (2000). Trade-offs in evolutionary immunology: Just what is the cost of immunity? *Oikos*, *88*(1), 87–98.

Luijckx, P., Ben-Ami, F., Mouton, L., Pasquier, L. D., & Ebert, D. (2010). Cloning of the unculturable parasite *Pasteuria ramosa* and its

Daphnia host reveals extreme genotype-genotype interactions. *Ecology Letters*, *14*(2), 125–131.
Luong, L. T., Horn, C. J., & Brophy, T. (2017). Mitey costly: Energetic costs of parasite avoidance and infection. *Physiological and Biochemical Zoology*, *90*(4), 471–477.
Niklas, K. J., & Hammond, S. T. (2019). On the interpretation of the normalization constant in the scaling equation. *Frontiers in Ecology and Evolution*, *6*, 212.
Nilsson, J. (2002). Metabolic consequences of hard work. *Proceedings of the Royal Society of London B: Biological Sciences*, *269*(1501), 1735–1739.
Nørgaard, L. S., Ghedini, G., Phillips, B. L., & Hall, M. D. (2021). Energetic scaling across different host densities and its consequences for pathogen proliferation. *Functional Ecology*, *35*(2), 475–484.
Nørgaard, L. S., Phillips, B. L., & Hall, M. D. (2019a). Can pathogens optimize both transmission and dispersal by exploiting sexual dimorphism in their hosts? *Biology Letters*, *15*(6), 20190180.
Nørgaard, L. S., Phillips, B. L., & Hall, M. D. (2019b). Infection in patchy populations: Contrasting pathogen invasion success and dispersal at varying times since host colonization. *Evolution Letters*, *91*(5), 555–566.
Olito, C., White, C. R., Marshall, D. J., & Barneche, D. R. (2017). Estimating monotonic rates from biological data using local linear regression. *Journal of Experimental Biology*, *220*(5), 759–764.
Olive, A. J., & Sassetti, C. M. (2016). Metabolic crosstalk between host and pathogen: Sensing, adapting and competing. *Nature Reviews. Microbiology*, *14*(4), 221–234.
Pettersen, A. K., Marshall, D. J., & White, C. R. (2018). Understanding variation in metabolic rate. *Journal of Experimental Biology*, *221*(Pt 1), jeb166876.
Råberg, L., Graham, A. L., & Read, A. F. (2009). Decomposing health: Tolerance and resistance to parasites in animals. *Philosophical Transactions of the Royal Society, B: Biological Sciences*, *364*(1513), 37–49.
Rigby, M. C., Hechinger, R. F., & Stevens, L. (2002). Why should parasite resistance be costly? *Trends in Parasitology*, *18*(3), 116–120.
Ritz, C., Baty, F., Streibig, J. C., & Gerhard, D. (2015). Dose-response analysis using R. *PLoS ONE*, *10*(12), e0146021.
Robar, N., Murray, D. L., & Burness, G. (2011). Effects of parasites on host energy expenditure: The resting metabolic rate stalemate. *Canadian Journal of Zoology*, *89*(11), 1146–1155.
Ruhs, E. C., Martin, L. B., & Downs, C. J. (2020). The impacts of body mass on immune cell concentrations in birds. *Proceedings of the Royal Society B: Biological Sciences*, *287*(1934), 20200655.
Ruiz, T., Koussoroplis, A., Danger, M., Aguer, J., Morel-Desrosiers, N., & Bec, A. (2021). Quantifying the energetic cost of food quality constraints on resting metabolism to integrate nutritional and metabolic ecology. *Ecology Letters*, *24*(11), 2339–2349.
Sandland, G. J., & Minchella, D. J. (2003). Costs of immune defense: An enigma wrapped in an environmental cloak? *Trends in Parasitology*, *19*(12), 571–574.
Sauer, E. L., Trejo, N., Hoverman, J. T., & Rohr, J. R. (2019). Behavioural fever reduces ranaviral infection in toads. *Functional Ecology*, *33*(11), 2172–2179.
Schmid-Hempel, P. (2003). Variation in immune defence as a question of evolutionary ecology. *Proceedings of the Royal Society B: Biological Sciences*, *270*(1513), 357–366.
Schmid-Hempel, P. (2011). *Evolutionary parasitology*. Oxford University Press.
Schmid-Hempel, P., & Ebert, D. (2003). On the evolutionary ecology of specific immune defence. *Trends in Ecology & Evolution*, *18*(1), 27–32.
Schmidt-Nielsen, K. (1990). *Animal physiology: Adaptation and environment*. Cambridge University Press.
Sheldon, B. C., & Verhulst, S. (1996). Ecological immunology: Costly parasite defences and trade-offs in evolutionary ecology. *Trends in Ecology & Evolution*, *11*(8), 317–321.
Siva-Jothy, M. T., Moret, Y., & Rolff, J. (2005). Insect immunity: An evolutionary ecology perspective. *Advances in Insect Physiology*, *32*, 1–48.
Steyermark, A. C. (2002). A high standard metabolic rate constrains juvenile growth. *Zoology*, *105*(2), 147–151.
Wang, A., Huen, S. C., Luan, H. H., Yu, S., Zhang, C., Gallezot, J.-D., Booth, C. J., & Medzhitov, R. (2016). Opposing effects of fasting metabolism on tissue tolerance in bacterial and viral inflammation. *Cell*, *166*(6), 1512–1525.e12.
White, C. R., Alton, L. A., Bywater, C. L., Lombardi, E. J., & Marshall, D. J. (2022). Metabolic scaling is the product of life-history optimization. *Science*, *377*(6608), 834–839.
White, C. R., & Kearney, M. R. (2014). Metabolic scaling in animals: Methods, empirical results, and theoretical explanations. *Comprehensive Physiology*, *4*(1), 231–256.
White, C. R., Kearney, M. R., Matthews, P. G. D., Kooijman, S. A. L. M., & Marshall, D. J. (2011). A manipulative test of competing theories for metabolic scaling. *The American Naturalist*, *178*(6), 746–754.
Yashchenko, V., Fossen, E. I., Kielland, Ø. N., & Einum, S. (2016). Negative relationships between population density and metabolic rates are not general. *Journal of Animal Ecology*, *85*(4), 1070–1077.
Zuk, M., & Stoehr, A. M. (2002). Immune defense and host life history. *The American Naturalist*, *160*(Suppl 4), S9–S22.

SUPPORTING INFORMATION

Additional supporting information can be found online in the Supporting Information section at the end of this article.

Figure S1: Variation in body mass for control, exposed and infected and exposed and uninfected animals.

Figure S2: The log–log relationship between metabolic rate and body mass.

Table S1: Linear mixed-effects analysis of covariance for the log–log change in metabolic rates.

Table S2: Analysis of variance for the energy use of a host before and after pathogen exposure.

How to cite this article: Hall, M. D., Phillips, B. L., White, C. R., & Marshall, D. J. (2024). The hidden costs of resistance: Contrasting the energetics of successfully and unsuccessfully fighting infection. *Functional Ecology*, *00*, 1–10. https://doi.org/10.1111/1365-2435.14523